phys. stat. sol. (b) 173, 661 (1992)

Subject classification: 71.55; 73.60; S7.12

Fachbereich Physik der Humboldt-Universität zu Berlin[1]) *(a)*,
Paul-Drude-Institut für Festkörperelektronik, Berlin[2]) *(b)*, *and*
University of Delaware, Material Science Program, Newark[3]) *(c)*

Ti Deep-Level Delta-Doping in GaAs Schottky Diodes: Capacitance–Voltage Analysis

By

J. PIPREK[4]) (a), P. KRISPIN (b), H. KOSTIAL (b), C. H. LANGE (b), and K. W. BÖER (c)

Deep-level Ti centers delta-doped within Al/n-GaAs Schottky diodes are investigated by CV-analysis. CV-profiles are modeled as a function of deep-level energy and local center distribution using 1D device simulation. The deep-level analysis is applied to MBE-grown GaAs samples with almost delta-like Ti doping (half-width 12 nm) yielding a double peak structure of the GV-profile. Besides the well-known Ti acceptor level in GaAs a yet unknown deeper level at about $E_c - E_t = 0.5$ eV is observed.

Es wird die Delta-Dotierung tiefer Störstellen in der Raumladungsrandschicht von Al/n-GaAs-Schottky-Dioden betrachtet und das effektive CV-Profil freier Ladungsträger als Funktion der Aktivierungsenergie und räumlichen Lage der Delta-Dotierschicht unter Benutzung einer 1D-Simulation berechnet. Mittels Molekularstrahlepitaxie werden Titan-Atome, die in GaAs bekannte tiefe Störstellen verursachen, als Delta-Verteilung mit einer Halbwertsbreite von 12 nm in n-leitende GaAs-Schichten eingebaut. Das CV-Profil enthält zwei Maxima, die dem Titan-Akzeptorniveau bei $E_c - 0.2$ eV und einem bisher nicht bekannten Defektterm bei $E_c - 0.5$ eV zugeordnet werden.

1. Introduction

Deep-level analysis is usually performed by deep level transient spectroscopy (DLTS) where the edge of a space charge layer is used to investigate kinetically active traps in a nearly homogeneously doped sample. Additional information is expected to be obtained when the deep-level doping is done in a single atomic layer (delta-doping) and the position of this layer is shifted from sample to sample with respect to the metallurgical interface of a pn-junction or the metal–semiconductor interface of a Schottky barrier. This permits a different n/p-ratio at the position of the center hence a differentiation between differently charged centers, and a more precise identification of complexes based on specific deposition methods. This knowledge is important, since the performance of most electronic devices is influenced by recombination via deep-level defects. In space charge regions deep-level recombination depends on the local position of the deep center corresponding to the spread of the quasi-Fermi level, i.e., on the deviation of the local carrier concentrations $n(x)$ and $p(x)$ from equilibrium. In most devices, little is known about the nature of the dominant deep-level defect which determines the minority carrier lifetime. The classical description of this recombination is based on the Shockley-Read-Hall (SRH) statistics [1]. Without detailed knowledge of the physical recombination mechanism, the process is described by

[1]) Invalidenstr. 110, O-1040 Berlin, Federal Republic of Germany.
[2]) Hausvogteiplatz 5–7, O-1086 Berlin, Federal Republic of Germany.
[3]) Newark, DE 19716, USA.
[4]) On leave at the University of Delaware, Material Science Program.

kinetic parameters of the deep level such as its concentration, its capture cross sections for electrons and holes (s_n and s_p), and its energy E_r.

This paper describes a first contribution to the proposed method by introducing a delta-doped layer separated from a Schottky barrier at a distance at which the edge of the space charge region can be moved across the layer with increasing reverse bias.

Many transition metal impurities in III–V semiconductors introduce deep levels in the energy gap. Ti doping of GaAs or InP leads to a semi-insulating material. It has the advantage of low diffusivity compared to other transition metals [2]. We have therefore chosen Ti in GaAs as our first deep-level dopant for experimental analysis. Substitutional Ti causes two levels in the gap of GaAs [3]: The Ti^{2+}/Ti^{3+} acceptor level at $E_c - 0.20$ eV, that acts as an electron trap having a negative charge state when occupied, and a neutral charge state when empty. Its cross section for electron capture at high temperature is $s_n^{\infty} \approx 3 \times 10^{-16}$ cm^2 and it is hardly changed at room temperature [4]. The cross section for hole capture of this center is unknown, but is probably in the range of $s_p \approx 10^{-14}$ cm^2 due to Coulomb attraction. The Ti^{3+}/Ti^{4+} donor level at $E_c - 0.87$ eV is neutral when occupied by an electron or positively charged when empty. The cross sections for this state at room temperature are $s_n \approx 10^{-14}$ cm^2 for electron capture and $s_p \approx 10^{-15}$ cm^2 for hole capture.

CV-analysis of shallow level delta-doping – at high doping densities to obtain quantum effects – is well-known and is dominated by carrier release from the quantum well (see, e.g. [5]). We apply CV-analysis on delta-doped deep levels at doping densities below 10^{11} cm^{-2} in order to investigate deep level properties and to avoid quantum-well effects.

Section 2 reviews briefly the employed modeling software PC-1D and the introduced improvements of physical models that are needed for the CV-analysis. In Section 3 the molecular beam epitaxy (MBE) is described for manufacturing the n-type GaAs samples, that are delta-doped with Ti, and metallized with an Al contact to form the Schottky barrier. In Section 4 computed CV-profiles are discussed, varying the energy position of the deep level and its local distribution. In Section 5 these results are compared with the measured CV-profile of the GaAs sample.

2. Models for Simulation

The PC-1D software package was originally developed for silicon solar cell simulation [6], using the finite-element analysis to solve the fully-coupled two-carrier semiconductor transport equations in one dimension. The two transport equations contain drift and diffusion for electrons and holes with a field- and doping-dependent mobility. The continuity equations take into account SRH statistics to model thermal generation and recombination and an additive optical generation term. The Poisson equation contains free carriers and the charges in shallow donors and acceptors.

The delta-doped sheet is considered by an appropriate interface boundary condition. The deep center is specified by its energy level E_r and by the recombination velocities S_n and S_p at the interface according to $S = s v_{rms} N_r$ with s the capture cross section, v_{rms} the thermal velocity (in GaAs: 4.6×10^7 cm/s for electrons and 1.6×10^7 cm/s for holes), and N_r the two-dimensional recombination center density. For a delta-doped sheet these centers act as interface levels, the reciprocal recombination velocities $1/S$ replace the lifetimes in the usual SRH rate yielding a two-dimensional recombination rate (dimension s^{-1} cm^{-2}).

We have then introduced into the source of PC-1D a donor- and an acceptor-like charge state of the recombination center, using the SRH occupation rate

$$f_r = \frac{S_n n + S_p n_i \exp\left(\frac{E_i - E_r}{kT}\right)}{S_n\left(n + n_i \exp\left(\frac{E_r - E_i}{kT}\right)\right) + S_p\left(p + n_i \exp\left(\frac{E_i - E_r}{kT}\right)\right)} \tag{1}$$

with the intrinsic density $n_i = 2.1 \times 10^6\ \mathrm{cm}^{-3}$ and the intrinsic level $E_i = E_c - 0.67$ eV for GaAs.

For simplicity, we assume in the theoretical analysis of Section 4 only one deep level. In general, both levels of the Ti center in n-GaAs can serve for recombination [7] and are taken into account for fitting the measurement in Section 5. The recombination velocities S_n and S_p of each Ti level depend on the occupation rate of the other level (A and D for acceptor- and donor-like state, respectively),

$$S_A = s_A v_{rms} N_r f_D \quad \text{and} \quad S_D = s_D v_{rms} N_r (1 - f_A); \tag{2}$$

this assumes that the level A exists only when D is occupied, and that D is not available for recombination when A is occupied. It excludes recombination traffic between both levels [8]. The one-level SRH recombination rate U is then replaced by the sum of the corresponding rates U_A and U_D.

The electron and hole mobilities are assumed to depend on the gradient of the corresponding quasi-Fermi levels, i.e., on the electrochemical fields denoted by F_n and F_p, respectively, which we have used as representing the external field component [9]. For the case of GaAs, the electron mobility is introduced as [10]

$$\mu_n = \frac{\mu_{n0} + v_n^*\left(\frac{F_n^3}{F_c^4}\right)}{1 + \left(\frac{F_n}{F_c}\right)^4} \tag{3}$$

because of electron scattering into the side valley of the conduction band at higher electric fields. The critical field of this process is $F_c = 4$ kV/cm; the drift saturation velocity in GaAs is $v_n^* = 8.5 \times 10^6$ cm/s.

Input and output of PC-1D have been extended for the needs of our investigations. Specifically we have included the display of the total space charge Q as function of the applied voltage in order to perform CV-analysis.

3. Experimental Setup

GaAs samples were grown by molecular beam epitaxy (MBE) in a multi-chamber system. High-purity elemental sources of gallium (7N), arsenic (6N), and silicon were used for growth onto semi-insulating GaAs (001) substrates that were misoriented 2° towards (111) Ga. Titanium (4N) was evaporated from a titanium filament. The 1 inch GaAs wafers were mounted with indium on the molybdenum substrate holder after chemical surface preparation and thermal oxidization by a procedure outlined in [11]. RHEED intensity oscillations of the specular beam were monitored prior to the growth to calibrate the growth rate.

GaAs was deposited at a substrate temperature of 540 °C and a rate of 0.5 μm/h. The arsenic flux was set to provide a clear (2 × 4) surface reconstruction for the GaAs growth [12].

The growth sequence of the individual layers in the structure is as follows: 500 nm of undoped GaAs as buffer layer, about 300 nm of n-type GaAs doped with silicon, planar deposition of titanium during interruption of the Ga and Si flux and then followed by about 250 nm of silicon-doped GaAs. The silicon flux has been chosen to give an electron concentration in the 10^{16} cm^{-3} range. The amount of titanium was varied by an empirically determined time and temperature program of the filament.

The distribution of the incorporated titanium atoms was analyzed by secondary ion mass spectroscopy (SIMS). Fig. 1 shows the SIMS profile of the Ti distribution of sample M1134, considered in the following discussion, with a sharp Ti peak of half-width 12 nm at 288 nm below the Al/GaAs interface. Some Ti atoms are floating on the MBE crystallization front, yielding a shoulder up to 100 nm from the main peak. The integral Ti density is about 2×10^{13} cm^{-2} – much higher than the intended value of 10^{11} cm^{-2}. However, only a small fraction of the Ti atoms is active as charged recombination centers (see below). Quantum-well effects caused, e.g., by tunneling of carriers into the quantum well with consequently altered recombination are not to be expected in our n-type sample because negatively charged Ti centers are screened by the space charge of unoccupied fixed Si donors, while free holes are not available in a sufficient amount. This is in contrast to shallow acceptor delta-doping, where the acceptors release holes to form a quantized two-dimensional hole gas in the valence band.

In order to apply the CV-method, a quasi-ohmic contact at the periphery of the sample and a Schottky contact at the center top were used. For the Schottky barrier, an Al film was deposited in a separate vacuum system. This causes a potential barrier of about 0.77 eV (Al/GaAs contact potential: 0.72 eV) and a space charge layer width $W \approx 150$ nm adjacent to the Al/n-GaAs Schottky contact. At zero applied voltage the delta-doped sheet lies outside of the space charge region. Fig. 2 displays the corresponding energy band diagram, and Fig. 3 the distribution of charged shallow Si donors with 3×10^{10} cm^{-2} Ti centers at 250 nm. Without bias both Ti levels are occupied by electrons resulting in a negative charge

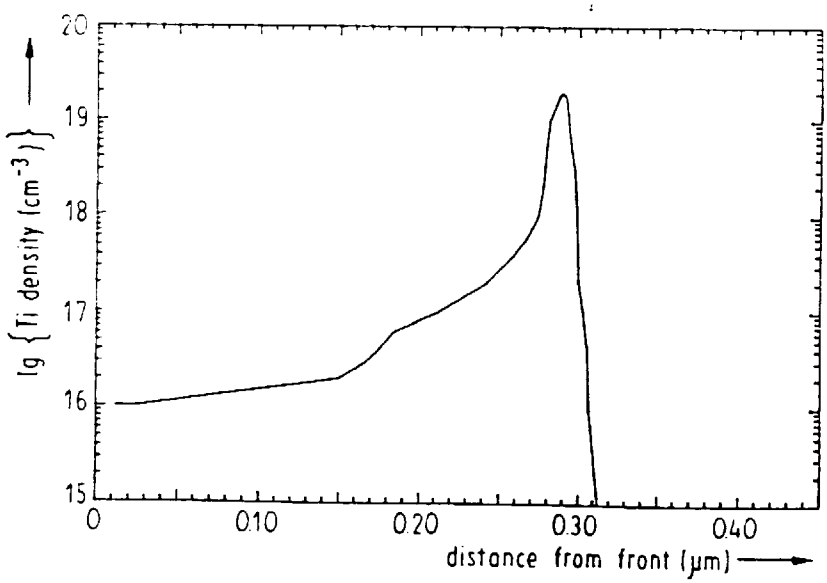

Fig. 1. Measured SIMS profile of the Ti distribution in sample M1134 (total Ti density: 2×10^{13} cm^{-2}, peak position: 288 nm, peak half width: 12 nm)

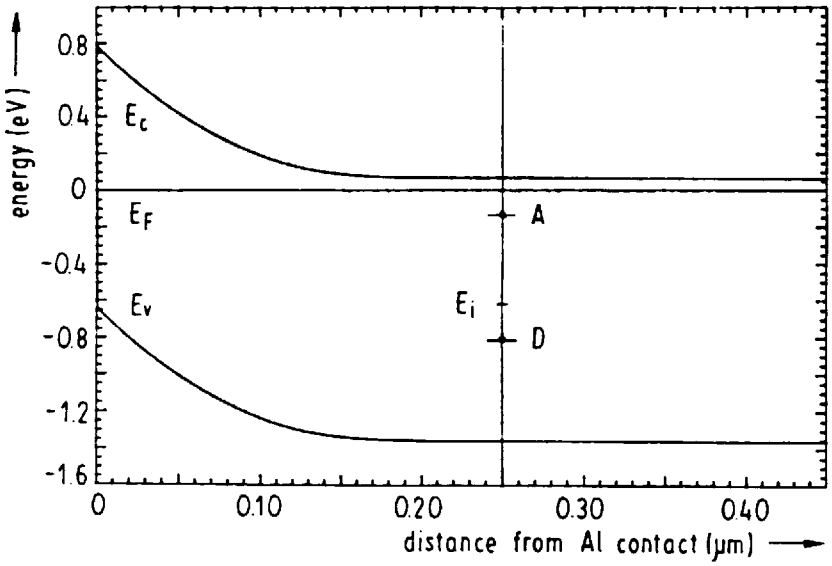

Fig. 2. Zero bias energy band diagram of the Al/n-GaAs Schottky contact showing the acceptor-like (A) and donor-like (D) deep level of the Ti center delta-doped in a distance of 250 nm from the metal (conduction band edge E_c, valence band edge E_v, Fermi level E_F, intrinsic level E_i)

state of the center. The corresponding positive screening charges, i.e. unoccupied silicon donors surround the Ti centers. The Debye screening length is $L_D = 22$ nm at room temperature for the used doping of $N_D = 4 \times 10^{16}\,\mathrm{cm}^{-3}$ in GaAs.

4. Capacitance–Voltage Analysis

With increasing reverse bias the band edges in Fig. 2 are lifted, and at a certain applied voltage the Ti acceptor level crosses the Fermi level and becomes discharged. The deep-level discharge causes a change of the total space charge Q of the Schottky contact and can be seen in the CV-characteristic ($C = |\mathrm{d}Q/\mathrm{d}V|$). Fig. 4 displays the influence of the Ti centers on the CV-characteristic (solid curve) in comparison to the sample without delta-doping (dashed curve): with raising reverse bias the width of the space charge region increases and

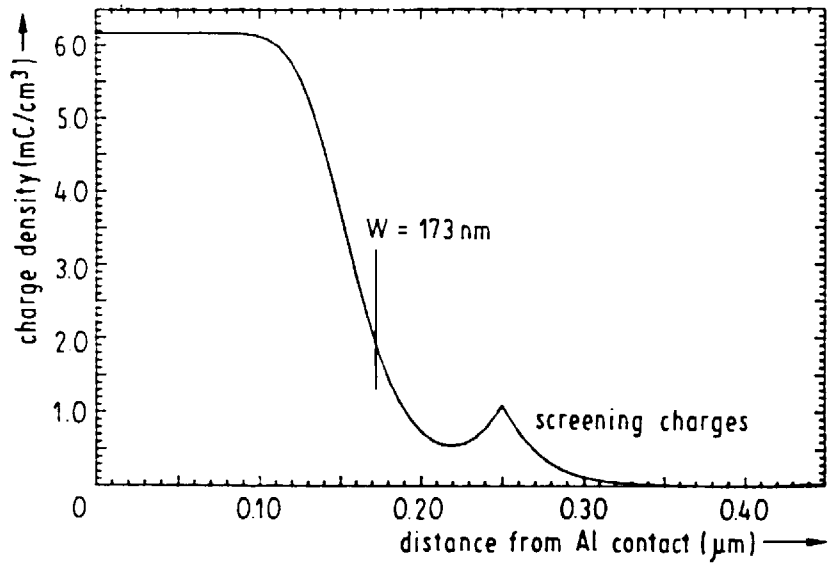

Fig. 3. Space charge distribution of unoccupied shallow Si donors according to Fig. 2 with a Ti center density of $3 \times 10^{10}\,\mathrm{cm}^{-2}$ (depletion width $W = \varepsilon\varepsilon_0/C$)

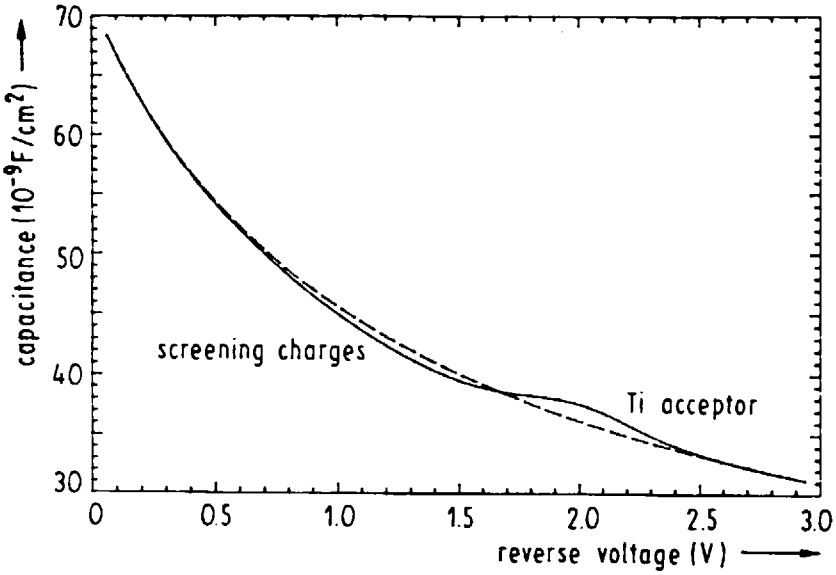

Fig. 4. Modeled CV-characteristics of the Al/n-GaAs Schottky contact without deep centers (dashed) and with 3×10^{10} cm^{-2} Ti centers (solid), delta-doped at 250 nm (Fig. 2)

it absorbs first the positive screening charges, causing a reduction of the capacitance. At still higher reverse bias, the negative charges of the Ti acceptor level are released, causing a higher capacitance. The usual CV-analysis [13] calculates carrier densities $N_{CV} = (2C^3/e\varepsilon\varepsilon_0)\,(dC/dV)^{-1}$ with e the elementary charge and $\varepsilon = 12.9$ the static dielectric constant of GaAs. Without delta-doping of deep centers this carrier density N_{CV} remains constant and is equal to the density N_D of shallow Si donors (dashed curve in Fig. 5). With deep level centers (solid curve in Fig. 5) an N_{CV}-minimum emerges first due to already charged Si donors that are screening the Ti centers. The position of that first minimum is influenced by the density of charged deep levels and is given by the position of the space charge edge shown in Fig. 3 at a voltage at which the Si screening charge peak just disappears. This position can be substantially different from the local Ti position. The discharging of

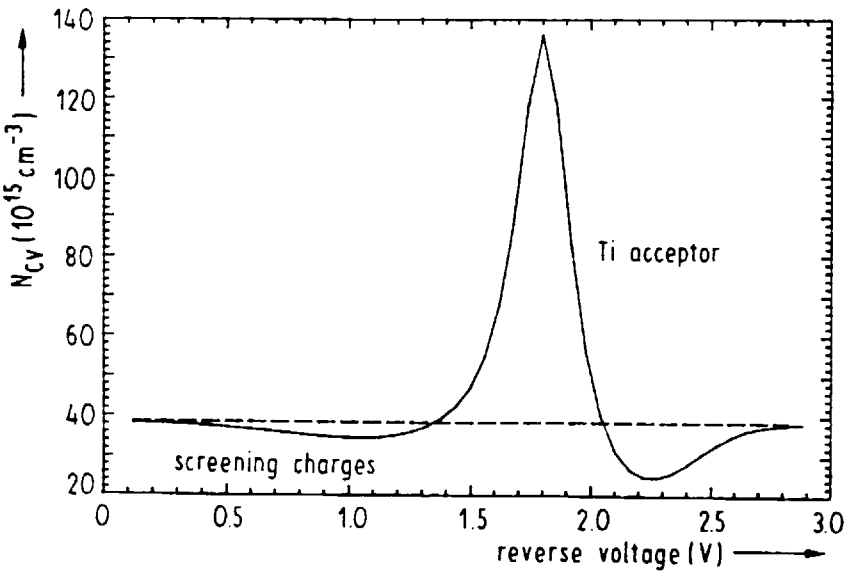

Fig. 5. Carrier density $N_{CV}(V)$ from the CV-characteristics in Fig. 4 giving the density of shallow donors in the case without deep levels (dashed) and exhibiting strong effects in the case with Ti delta-doping (solid)

the delta-doped Ti acceptor level produces a sharp N_{CV}-peak. A donor-like level would result in an identical peak, because the total space charge rises by the same amount, and can be distinguished from an acceptor only by the missing first N_{CV}-minimum. The N_{CV}-peaks is the higher the smaller dC/dV is. A second minimum calculated at 320 nm and shown in Fig. 5 is related to the second turning point of the solid curve in Fig. 4 during deep level discharge.

In the following figures, the density N_{CV} is plotted versus the depletion width $W = \varepsilon\varepsilon_0/C$, as obtained from classical CV-analysis [13]. In our case the capacitance C is influenced by the deep level, causing little deviations of the calculated W from the position of the space charge front (see Fig. 3). However, the W-value of a deep-level peak in $N_{CV}(W)$-profiles is always higher than the local position of the deep center, and it increases with larger energy distance of the deep level from the conduction band edge. A local shift of the delta-doped sheet causes a corresponding local shift of the $N_{CV}(W)$-profile.

Deep-level peaks in $N_{CV}(W)$-profiles are determined by the change of the SRH occupation rate f_r with increasing reverse bias, i.e., with decreasing majority carrier density $n(x)$ and increasing minority carrier density $p(x)$. At low reverse voltage, $n(288\text{ nm}) \gg n_i \gg p(288\text{ nm})$ is fulfilled and the Ti acceptor peak in Fig. 5 does not depend on the capture cross sections for electrons and holes (See (1)). Therefore, the physical recombination mechanism via this Ti acceptor level can only be investigated with the presented CV-analysis in a pn-junction when the delta-doped sheet is incorporated at a position at which $n \approx p$ can be established.[5]) With deeper recombination levels a larger reverse bias is needed for discharging, causing a shift of the $N_{CV}(W)$-peak towards higher W (Fig. 6). The N_{CV}-peak increases because $d^2n(288\text{ nm})/dV^2$, dominating dC/dV, decreases with higher reverse bias. When the depth of the recombination level approaches the intrinsic level, the discharging is not complete because the occupation rate saturates at a finite value. This can be shown by setting $E_r = E_i$ and $S_n = S_p$ in (1). Thus, the peaks become smaller with still deeper recombination centers and disappear totally when the level lies about 0.1 eV below E_i.

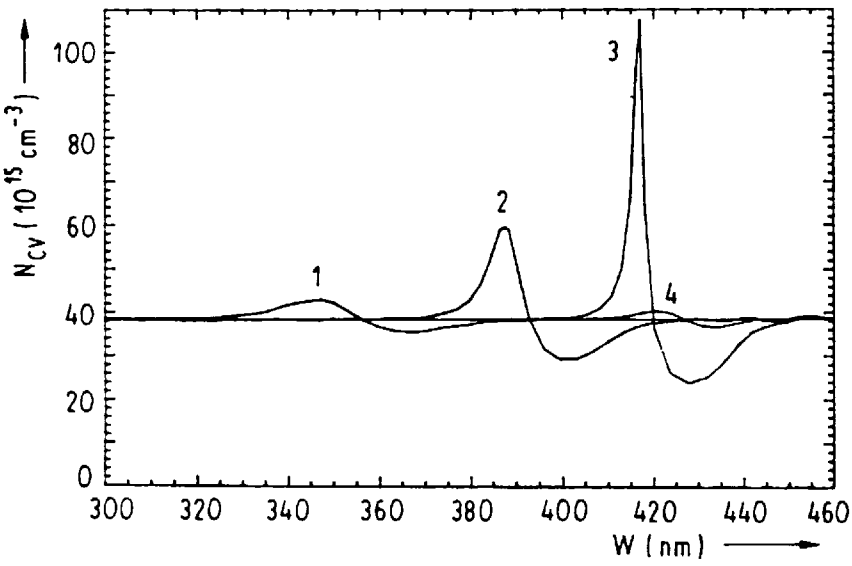

Fig. 6. Calculated CV-profiles $N_{CV}(W)$ with 3×10^9 cm^{-2} Ti centers at 288 nm varying the energy $E_c - E_r$ of the acceptor level: (1) 0.2, (2) 0.4, (3) 0.6 eV, and (4) $E_r = E_i$

[5]) An interesting effect that could be investigated with this method was described in [14].

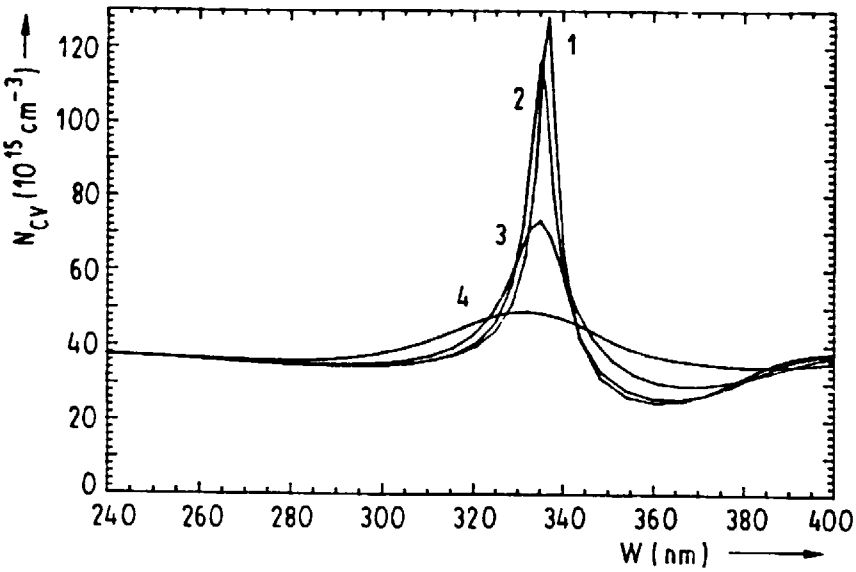

Fig. 7. Calculated CV-profiles $N_{CV}(W)$ with 3×10^{10} cm^{-2} Ti centers comparing the two-dimensional Ti sheet at 288 nm (1) with a Gaussian broadening of the Ti center distribution having a half-width of (2) 12, (3) 25, and (4) 50 nm

The influence of a Gaussian broadening of the Ti deep center distribution is investigated in Fig. 7. For the family of curves the total center density is kept constant. The half-width of 12 nm corresponds to the SIMS measurement of the total distribution of Ti atoms and causes only minor deviation from a strictly two-dimensional center distribution. With increasing half-width, the N_{CV}-peak due to Ti acceptor discharge becomes smoother and the calculated second N_{CV}-minimum starts to vanish.

5. Comparison with Measurement

The measured CV-profile $N_{CV}(W)$ of the delta-doped Schottky diode shows the depletion of carriers near $W = 250$ nm and two peaks at 340 and 407 nm (solid curve in Fig. 8). The

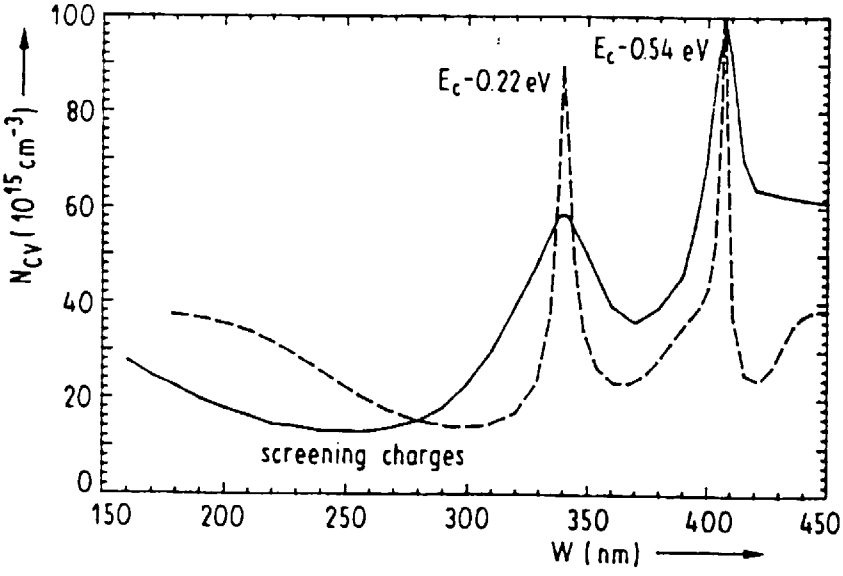

Fig. 8. Measured (solid) and computed (dashed) CV-profile $N_{CV}(W)$ of sample M1134. Simulation with deep levels at 0.22 and 0.54 eV below the conduction band in 288 nm distance to the metal contact (free electron density 4×10^{16} cm^{-3}, depletion density 3×10^{11} cm^{-2}, barrier height 0.77 eV)

shallow dopant density cannot be clearly identified from the measurement. A value of $N_D = 4 \times 10^{16}\,cm^{-3}$ is assumed, corresponding to the zero bias depletion width of 160 nm [13]. Thus, an integral value of $3 \times 10^{11}\,cm^{-2}$ screening charges is deduced from Fig. 8. This value is much smaller than the total density of $2 \times 10^{13}\,cm^{-2}$ Ti atoms, as obtained from SIMS measurement (Fig. 1). Consequently, only about 1% of the Ti introduced by MBE seems to be charged at zero bias. Because of the well-known gettering properties of Ti, the formation of complex Ti centers that cannot be discharged and composed of several Ti atoms or other impurities and intrinsic defects is probable. Another possibility are fixed screening charges that cannot be seen in the CV-profile.

In the attempt to fit our simulated $N_{CV}(W)$-characteristic (dashed curve in Fig. 8) with the experimental curve, we obtain the measured peak positions with two deep levels at 288 nm and energy values of 0.22 and 0.54 eV below E_c. The first one is in good agreement with the published value of the Ti acceptor level. The second level might be connected with a so far unknown complex Ti center mentioned above. The amplitude of the peaks depends on the frequency of the CV-measurement (here 100 kHz) and cannot be analyzed in the quasistatic simulation.

The expected donor level at $E_D = E_c - 0.87\,eV$ is too deep to be accessible with the present analysis. For an Al/GaAs barrier height of 0.77 eV the Ti donor level cannot cross the Fermi level and therefore cannot be discharged, hence is not seen in the CV-measurement. With higher metal–semiconductor contact potential the Ti donor level ist still not accessible: when E_D crosses the electron quasi-Fermi level at high reverse bias, both carrier densities at 288 nm are much smaller than $n_i \exp((E_i - E_D)/kT) = 5 \times 10^9\,cm^{-3}$ and therefore the occupation rate remains $f_r \approx 1$.

The calculated N_{CV}-minimum due to mobile screening charges occurs somewhat below 300 nm in contrast to the measured one at 250 nm. This discrepancy supports the hypothesis of additional screening charges fixed in other deep level defects.

6. Conclusions

Deep-level delta-doping in Schottky diodes causes characteristic structures in the CV-profile which can be used to determine the energy position of the deep level, its acceptor-like or donor-like type, and the density of charged centers. The CV-analysis of first samples of MBE-grown GaAs with almost delta-like sheets of Ti centers features, besides the well-known Ti acceptor level, a so far unknown deep level at about $E_c - 0.5\,eV$ which is probably caused by complex Ti defects. Further experiments are planned to identify the origin of the additional level.

Acknowledgements

One author (J.P.) was partially supported by the Deutsche Forschungsgemeinschaft DFG. The authors acknowledge the technical assistance of Mrs. K. Hagenstein.

References

[1] W. Shockley and W. T. Read, Jr., Phys. Rev. **87**, 835 (1952).
R. N. Hall, Phys. Rev. **87**, 387 (1952).
[2] H. Ullrich, A. Knecht, D. Bimberg, H. Kräutle, and W. Schlaak, J. appl. Phys. (1992), to be published.
[3] H. Scheffler, W. Korb, D. Bimberg, and W. Ulrici, Appl. Phys. Letters **57**, 1318 (1990).

[4] C. D. Brandt, A. M. Hennel, T. Bryskiewicz, K. Y. Ko, L. M. Pawlosicz, and H. C. Gatos, J. appl. Phys. **65**, 3459 (1989).
[5] E. F. Schubert and K. Ploog, Japan. J. appl. Phys. **25**, 966 (1986).
[6] P. A. Basore, IEEE Trans. Electron Devices **37**, 337 (1990).
[7] J. Piprek, H. Kostial, P. Krispin, C. Lange, and K. W. Böer, in: Physics and Simulation of Optoelectronic Devices, Ed. by D. Yevick, Proc. SPIE **1679**, 232 (1992).
[8] A. Zunger, private communication.
[9] K. W. Böer, Survey of Semiconductor Physics, vol. II, Van Nostrand Reinhold, New York 1992 (pp. 663, 664).
[10] S. Selberherr, Analysis and Simulation of Semiconductor Devices, Springer-Verlag, Wien 1984 (p. 97).
[11] H. Fronius, A. Fischer, and K. Ploog, J. Crystal Growth **81**, 169 (1987).
[12] L. Däweritz and R. Hey, Surface Sci. **236**, 15 (1990).
[13] S. M. Sze, Physics of Semiconductor Devices, Chap. 5.2, John Wiley & Sons, New York 1982.
[14] J. Piprek and A. Schenk, J. appl. Phys. **72**, No 12 (Dez. 1992), to be published.

(Received June 23, 1992)